The Spin Field-Effect Transistor: Can It Be Realized?

Hiwa Modarresi*
** Zernike Institute for Advanced Materials, University of Groningen, Nijenborgh 4, 9747 AG Groningen, the Netherlands*

Supervisor: Caspar van der Wal

(Submitted to Erik Van der Giessen: June 1st, 2009)

Abstract
If it is realized, the proposed spin field-effect transistor can revolutionize the way all existing transistor-based devices work through the implementation of a faster and a more efficient performance accompanied by other advantages like non-volatility of data storage, less heat generation, and smaller space occupation. It is now more than two decades that the question "can the spin field-effect transistor be realized or not?" has been directed to the scientific community. In this article we discuss the fundamental concepts needed in the realization of spin field-effect transistor and challenges facing this newly born field of study. We then deduce our conclusion based on some remarkable progresses made during the last two years which give hope that the realization of spin field-effect transistor is within reach despite the significant challenges that lay ahead.

Contents **Page Number**

1 Introduction 1
1.1 Introduction to Spin Field-Effect Transistor 1
1.2 Concepts of Electron's Spin 1
1.3 Data and Das' Proposed Spin Field-Effect Transistor 3
1.4 Spin Injection, Transport, and Detection 4
2 Spin Field-Effect Transistor: Concepts from a Device Point of View 7
2.1 Benefits of Utilizing Spin Field-Effect Transistor 7
2.2 Energy Band Diagram of Spin Field-Effect Transistor 8
2.3 Device Structures of Spin Field-Effect Transistor 10
3 Some Recent Advances in Spin Injection, Transport, and Detection 13
3.1 Spin Injection into Silicon 13
3.2 Tunable Spin Tunnel Contacts on Silicon 14
3.3 Spin Transport in GaAs 16
3.4 Spin Transport in Silicon 18
4 Conclusion 21
5 Acknowledgments 21
6 References 22

1 Introduction

1.1 Introduction to Spin Field-Effect Transistor

Over the past few decades, size of transistors has been tremendously reduced from a few centimeters to a few tens of nanometers. This trend in down scaling the device size has almost reached its ultimate physical limitation, challenging *Moore's Law* which has been valid for almost half a century. This fact rings a bell for the scientific society to pursue other alternative options to continue the miraculous trend of improving electronic devices. One of the most promising alternatives is to introduce electrons' spin into a new transistor configuration which can give high or low output current according to the relative orientation of its ferromagnet contacts and spin direction of electrons.

The idea of spin field-effect transistor sparked after Fert et al. [1] and Grunberg et al. [2] discovered the *giant magneto resistance* effect in magnetic multilayer systems in 1988. They found huge differences in current coming out of a magnetic and metallic multilayer system when the magnetic layers had the same or different directions of magnetization due to spin-dependent scattering of electrons. Shortly thereafter room temperature magnetic field sensors were made [3] using spin property which had much better performance than previously used *anisotropic magneto resistance* property.

Following the preliminary realization of the potential benefits of utilizing spin property, Datta and Das proposed an electron wave analog of the electro-optic light modulator in the late 1989 [4]. Most of the today's interest in this newly born field of study is motivated by their well-known proposed device which is now known as *spin field-effect transistor*. Since the very basics of this new field are based on spin of electrons in electronic devices, the name *Spintronics* which is the combination of the words *spin* and *electronics* is also sometimes used to refer to it.

However, despite almost two decades of comprehensive effort dedicated to the realization of the proposed spin field-effect transistor, it has not been made yet. This article aims at answering the question "why spin field-effect transistor has not been made yet? Or is it possible at all to make it?"

We start with an introduction to the concepts of electron spin and proposed spin field-effect transistor in the first chapter. In the second chapter, we look more into details of spin field-effect transistor from a device point of view. In the third chapter, we discuss some significant experiments done in the last two years. Finally in the conclusion we argue the prospective of making spin field-effect transistor considering all different efforts dedicated to it and obstacles ahead of it.

1.2 Concepts of Electron's Spin

Spin of electron is a fundamental property which originates from electron's spinning around its axis. Depending on the direction of the angular momentum that this spinning causes we can call them spin-up (↑) when the angular momentum is pointed up or spin-down (↓) when it is pointed downwards.

In giant magneto resistance effect which we mentioned shortly before, a huge change is observed in the amount of resistance facing current passing through a metal which is sandwiched between two ferromagnets. Namely, the following ratio for devices showing giant magneto resistance effect is huge.

$$GMR = \frac{R_{\uparrow\downarrow} - R_{\uparrow\uparrow}}{R_{\uparrow\uparrow}} \times 100 \quad (1)$$

In this equation *GMR* represents giant magneto resistance ratio, $R_{\uparrow\downarrow}$ is the resistance of the device when polarization of ferromagnets are anti-parallel, and $R_{\uparrow\uparrow}$ is the resistance of the device when polarization of ferromagnets are parallel.

Figure 1 (a) shows the configuration by which we can see the giant magneto resistance effect (when the spacer between two ferromagnets is metal). Here the current is flowing in x-direction through the device which in this case is a metal that is sandwiched between two ferromagnets. If the magnetizations of both ferromagnets are directed to one side, electrons encounter minimum resistance while they are scattered from the edges of metal-ferromagnet interfaces. On the other hand, if the magnetizations of ferromagnets are directed in opposite directions, electrons face a greater resistance because of more spin-dependent scattering.

Figure 1 (b) shows two different magneto resistance states (i.e., when the magnetization directions of ferromagnets are the same or opposite) in a simplified way. A big magneto resistance ratio (which corresponds to a large gap between maxima and minima in Figure 1 (b)) is vital for better detection of spin-polarized current.

After successful experiments on giant magneto resistance, another configuration later was introduced in which current passed through the device of Figure 1 (a) in y-direction. In this configuration the spacer is an insulator and the effect seen is called *tunneling magneto resistance*. If the directions of magnetization of two ferromagnets are the same, device resistance would be smaller than when the directions of magnetization of two ferromagnets are opposite to each other.

In this effect unlike the giant magneto resistance configuration (in which the spin-dependent scattering of electrons from the metal-ferromagnet interfaces are the main cause of big magneto resistance ratio in equation 1) the dominant cause of difference between two different states (i.e., when the magnetization directions are the same or opposite to each other) is the spin-dependent tunneling through the insulator. Tunneling magneto resistance yields three times bigger magneto resistance values at room temperature with respect to giant magneto resistance [5] and therefore it is a good choice in making room temperature electronic devices.

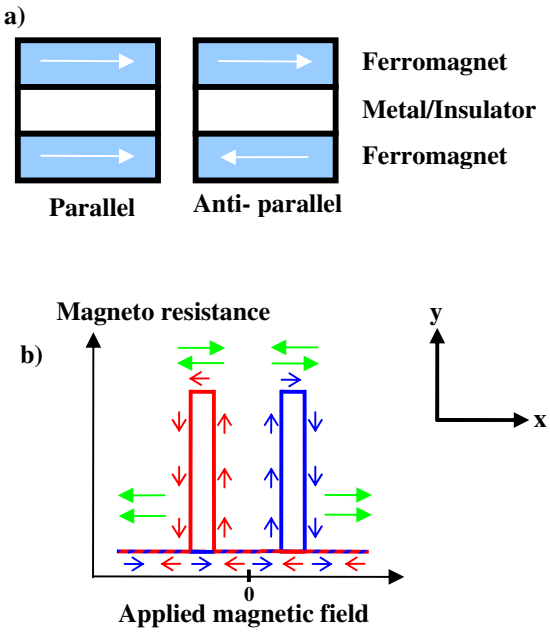

Figure 1 | (a) Device configuration of either *giant magneto resistance* or *tunneling magneto resistance* if the current is passed in x-direction (for a metal spacer) or y-direction (for an insulator spacer), respectively (b) A simplified picture showing the magneto resistance ratio for different magnetization directions (depending on the variation of external magnetic field).

In both giant magneto resistance and tunneling magneto resistance configurations, one ferromagnetic layer is usually made more susceptible to the external applied magnetic field than the other ferromagnetic layer via using different ferromagnets or

through shape anisotropy [6]. This allows us to control magnetization directions of different ferromagnetic layers with the applied magnetic field. Figure 1 (b) shows a simplified representation of dependence of magneto resistance on external applied magnetic field for both giant magneto resistance and tunneling magneto resistance. In the far left of this figure, magnetization directions of both ferromagnets are pointed to the left and therefore resistance of the device shows a minimum. We follow the blue arrows by decreasing the magnetic field down to zero and then switch the direction of the applied magnetic field and increase it until we change the magnetization direction of one of the ferromagnetic layer. At this moment we see a huge resistance in the device. By further increasing the external magnetic field we change the magnetization direction of the other ferromagnetic layer and we see again a small resistance in the device. We can repeat the same kind of experiment by following the red arrows from the far right in this figure i.e., by reducing and then reversing the direction of applied magnetic field. Doing this we would get a mirror like image of what we got in previous case.

Considering the fact that this device can show a large or small resistance for anti-parallel or parallel orientations of the magnetizations of ferromagnets, respectively, it can work as a valve and that is why this device is sometimes called *Spin Valve*.

1.3 Data and Das' Proposed Spin Field-Effect Transistor

In the late 1989 Supriyo Datta and Biswajit Das from Purdue University proposed an electron wave analog of the electro-optic light modulator [4]. Most of the today's interest in spintronics is motivated by their well-known proposed device which is now known as the spin field-effect transistor.

The idea was to extend the *on-off* states of light beam which depends on the direction of polarizer and analyzer and can be switched by manipulating an electro-optic cell (as it is shown in Figure 2) to the spin-dependent current of electrons. They proposed that a transistor can be made in which spin direction of electrons plays the most prominent role in the device output current. In their proposed transistor, electrons pass through ferromagnetic source and drain contacts and a semiconductor channel in which the spin direction of electrons can be manipulated (using the gate bias) to get the desired *on-off* states of the device.

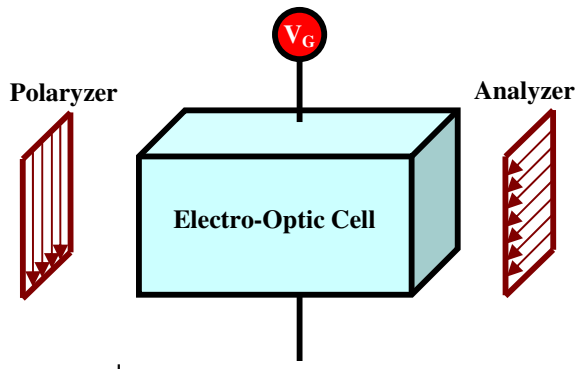

Figure 2 | Wave modulator can work as both light transmitter and light blocker depending on the voltage bias of the electro-optic cell. Two perpendicularly located polarizer and analyzer plates are located in both sides of the electro-optic cell. After light is polarized by polarizer it goes trough electro-optic cell and finally it meets the analyzer.

In a wave modulator if the incoming beam is polarized and then is passed through an electro-optic cell to reach the analyzer in a configuration which is shown in Figure 2, depending on the existence of electric field in electro-optic cell, light can pass the analyzer or can be blocked. This happens because electro-optic cell can rotate the angle of polarization of the light beam if it is biased by the proper voltage.

Datta and Das proposed that one can make an analogous device in which the electron's spin property is used instead of beam

polarization (a schematic of such a device is shown in Figure 3). In this device, the injected current into the semiconductor channel is spin selected. The fact that this current has a majority spin which are directed to one side is because the injected electrons come from the ferromagnetic source contact in which we do not have equilibrium between two spin states. Ferromagnets have a majority spin up or down which determines the magnetization direction of them.

Source contact can be considered as the analog of polarizer in an optical wave modulator since it can inject a majority spin up or down into the semiconducting channel. The electrons, most of which have the spins up or down, pass through a two dimensional electron gas (2DEG) inside the semiconductor channel. If the directions of majority spins can be aligned via gate bias to point to the same or opposite direction as of the ferromagnet drain contact, the device's conductance would be respectively high or low.

The spin direction of electrons can be manipulated by the gate voltage. The spin precession angle of the electrons in the semiconductor channel depends on the strength of applied voltage described by a phenomenon which is known as *Rashba effect*.

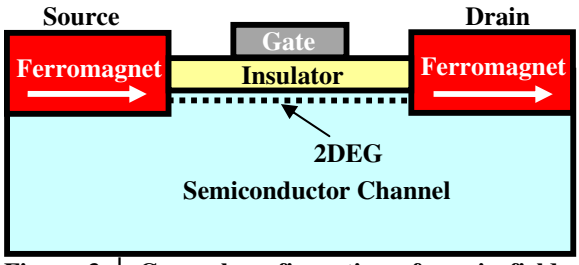

Figure 3 | General configuration of a spin field-effect transistor proposed by Datta and Das. Ferromagnetic source and drain contacts are located on two sides of a semiconductor channel in which spin-polarized current in two dimensional electron gas (2DEG) can be manipulated via gate voltage.

As it can be seen from Figure 3 the basic configuration of proposed device by Datta and Das is almost like today's transistors but it utilizes spin injection and detection properties in its source and drain contacts, respectively. When the magnetization direction of ferromagnetic drain is parallel to that of the majority spin orientation of the electrons at the drain side of the channel, the current can flow through the drain and thus the *on*-state of the spin field-effect transistor is created. By changing the gate voltage the angle of spin precession changes through Rashba effect. Using this property one can induce the preferred alignment to the spins of electrons in semiconducting channel. When the spin alignment between the electrons at the channel end (next to the drain contact) is anti-parallel to the magnetization direction of the drain itself, electrons cannot pass through the device anymore and the drain current drops sharply because of the magneto resistive nature of this phenomenon. This situation in which the output current is decreased sharply can be interpreted as the *off*-state of the spin field-effect transistor. Changing the gate voltage gives cyclic *on-off* states because of different precession angles which are created with respect to different applied gate voltages.

1.4 Spin Injection, Transport, and Detection

In order to realize a device working on the basis of spin, namely spin field-effect transistor, three major requirements should be satisfied. The first requirement is the injection of spin-polarized current of electrons from ferromagnetic source into semiconductor. The second one is the transport of electrons through the semiconductor channel without losing the spin direction. And the third requirement is the detection of spin-dependent transmission into the ferromagnetic drain contact.

Even overcoming the first requirement is by itself a big challenge and it is not so straightforward to inject spin-polarized current into semiconductor by making a contact between a ferromagnetic metal and a semiconductor. A ferromagnetic metal contains an excess of electrons whose spins are directed to one side that forms the magnetization direction of the ferromagnet. One may expect that these imbalanced spin-polarized electrons can be injected into the semiconductor by applying a voltage to the ferromagnet metal-semiconductor contact. But in reality spin-polarized electrons cannot be injected from ferromagnetic metal into semiconductor in this way. This arises from the fact that conduction of ferromagnetic metal is by far bigger than that of semiconductor and any voltage applied to the ferromagnetic metal-semiconductor contact falls on the edges of semiconductor. Since the origin of this problem arises from the fact that conductance of different layers in the contact are different, this problem is known as *conductivity mismatch* [7]. In order to overcome this problem one can introduce a thin layer of insulator at the boundary between the ferromagnetic metal and semiconductor. This barrier provides a spin-dependent tunnel resistance that allows the spin injection into the semiconductor.

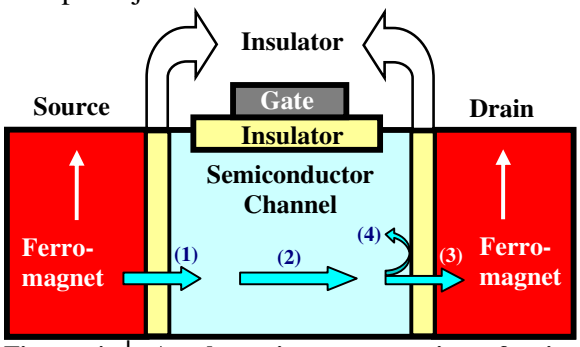

Figure 4 | A schematic representation of spin field-effect transistor consisting of a ferromagnetic source, a Semiconductor channel, and a ferromagnetic drain. An insulator is incorporated between different contacts and semiconductor channel. Cyan arrows show possible routs of electrons.

A schematic representation of different contacts to the semiconductor along with direction of spin-polarized current in spin field-effect transistor is shown in Figure 4. Arrow number (1) in this figure shows the direction of successfully injected spin-polarized electrons from ferromagnetic source contact into semiconductor channel through tunneling.

Meeting the second requirement that was mentioned in the beginning of this section (which deals with transport inside semiconductor channel) necessitates the transport of electrons in the channel while their spin direction is maintained (arrow number (2) in Figure 4 shows the spin-polarized current inside the semiconductor channel). If spin-polarized current moves through the semiconductor in a diffusive transport regime (in this kind of transport, electrons scatter continuously on their way through the lattice), we expect electrons to lose their spin direction after a short distance. This happens because of the fact that after each scattering it is more likely that electrons adopt a new spin direction and lose their original spin direction. In order to maintain the spin direction, electrons should travel through the semiconductor in a ballistic transport regime (in this kind of transport, electrons move inside the channel without any scatterings). This means that electrons should have the minimum number of scatterings as possible while moving from the source contact to the drain contact.

The rules governing the spin-dependent transmission (third condition) are almost the same as rules applied to spin-dependent injection that was explained earlier. Those common rules include the conductivity mismatch problem which should be addressed here again. Besides, in order to have a good output signal, one should raise the probability by which the spins are going from semiconductor channel into the ferromagnetic drain contact (arrow number

(3) in Figure 4). Otherwise, back scattered electrons (arrow number (4)) are more likely to lose their spin property and decrease the spin-up, spin-down ratio when electrons try again to pass through the barrier towards the ferromagnetic drain contact.

2 Spin Field-Effect Transistor: Concepts from a Device Point of View

2.1 Benefits of Utilizing Spin Field-Effect Transistor

It is now several decades that human effort has been focused on optimizing the size, speed, and power consumption of existing metal-oxide-semiconductor field-effect transistors (MOSFETs) or the so called charge based transistors. But why after all the progresses made in the field of charge based transistors, we are now pursuing to improve devices which work on the basis of spin transfer technology?

The first answer to this question can be discussed from an energy point of view when transistors are working in dynamic (active) mode. In order to continue marvelous progress in improving the device performance, the predicted switching energy (energy which is needed to switch between *on* and *off* states) by *international technology roadmap for semiconductors* in 2018 is *1500 eV/μm* [8]. The switching energy required for devices which work on the basis of charge transfer even for an imaginary gate width of *10 nm* (the smallest gate width reached so far is about *40 nm*), would be approximately three orders of magnitude larger than this amount [9]. On the other hand, the minimum switching energy for the spin field-effect transistor that Datta and Das proposed is only *23 meV* [10]. These numbers show a huge advantage of spin based transistors over present charge based devices.

The second reasoning is again from an energy point of view but this time for a situation in which transistors are working in their static mode (this time they are not switched between *on* and *off* states but they have to keep their *on-off* states). In spin based transistors the static power dissipation is reduced to zero due to their magnetic nature of data storage, while in present charge based devices the static power dissipation is a major challenge in improving transistor performance. Static power dissipation in charge based devices is due to source drain leakage and can be minimized by increasing the barrier (for example by increasing channel length). However, we now that this solution which aims at decreasing the static power dissipation, at the same time increases the dynamic power consumption of the device. This happens because when there is a higher barrier in the device, there should be a higher voltage applied to the contacts of the device that leads to higher power consumption.

In addition, spin based transistors can further down scale the transistor devices while the charge based devices already have reached their minimum limit of gate length which is approximately *40 nm*. This gives the third reason to the question made in the beginning of this section.

In order to better compare spin transfer devices with its currently mature charge transfer rival, here we explain the fundamental differences between the two devices in Figure 5. The left side of this figure shows the operation mechanism of a charge based transistor. In part (a) of the Figure 5 a barrier is raised to turn the drain current *off* while in part (b) of the Figure 5 this barrier is removed to have the current flowing to drain. Barrier has to be sufficiently high and thick to maintain a large *on-off* ratio for the drain current. A problem which arises in this kind of devices stems from the fact that the higher and thicker this barrier is the larger the threshold voltage, and thus, the larger the gate switching energy will be.

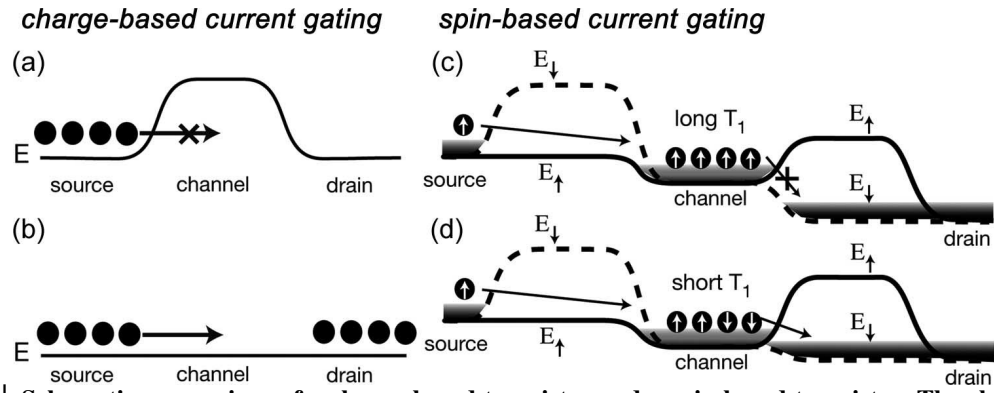

Figure 5 | Schematic comparison of a charge based transistor and a spin based transistor. The charge based transistor operates via controlling the height of the barrier, which is *up* in (a) and *down* in (b). The barrier height and width determine the *on-off current ratio* along with the *leakage current*. The spin based transistor operation is determined by the nature of the initial spin states moving through fixed barriers. If the carriers that are reaching the drain are fully spin-polarized, the transistor is in its *off* state (c) otherwise the transistor is in its *on* state (d). In this figure $E_{\uparrow}$ and $E_{\downarrow}$ show the barrier height facing spin-up and spin-down electrons, respectively, and T_1 is the spin lifetime [9].

The spin field-effect transistor does not function through lowering or raising a barrier as it is shown in Figure 5 (c) and (d) (for one version of the spin field-effect transistor which is mentioned in reference [11]). The barrier is identical in both *on* and *off* states of the device. Electrons of one spin see a large barrier while the electrons of the other spin see no barrier on their way. Therefore, electrons of one spin direction are injected into the channel region and they cannot go through the ferromagnetic drain contact unless their spins are flipped. If the spin lifetime (T_1) in the channel region is very long, the amount of current flowing out of ferromagnetic drain is very small, whereas if the spin lifetime in the channel region is short, then the ferromagnetic drain current output would be large.

Modification of the spin lifetime to a length appropriate for the *on*-state configuration in spin field-effect transistor requires a much smaller electric field than raising or lowering the barrier for the charge transfer transistor. Quantum mechanically measured a *1 meV* spin splitting can cause a spin to completely reorient by precession in only *1 ps* [9]. Generating this spin relaxation via applying an electric field to the gate of a spin transfer transistor and producing a Rashba field implies that a slightly larger voltage is required. For the structure mentioned in [11], $V_{th} \approx 100\ mV$ is enough to reduce the spin lifetime to *10 ps*.

2.2 Energy Band Diagram of Spin Field-Effect Transistor

The basic structure of a spin field-effect transistor is constructed from a metal oxide semiconductor (MOS) gate and two ferromagnetic contacts of source and drain, as it is shown in Figure 3 in the first chapter. We also know that the existence of an insulator layer between ferromagnets and semiconductor channel so far has shown a necessity to overcome the problem of conductivity mismatch. Having said that, a variety of band diagrams for different spin field-effect transistors are shown in Figure 6. Ferromagnetic p-n junctions using a ferromagnetic semiconductor and

ferromagnetic Schottky junctions using a ferromagnetic metal all can be employed as the source or drain of spin field-effect transistors. The *on-off* operation states of the spin field-effect transistor are based on the modification induced through the gate voltage by which the height or width of the barrier structure at the source-channel junction is slightly changed. Examples of these kinds of junctions are shown in Figure 6 (a) and Figure 6 (b). Here, the ferromagnetic source and drain act as spin injector and spin detector, respectively, and therefore the output current depends on the magnetization configurations of the source and drain and also on *spin relaxation length* (an average distance up to which electrons keep their spin directions intact).

Half-metallic ferromagnets are also useful for the ferromagnetic source and drain. The band structure of half-metallic ferromagnets is comprised of metallic and insulating or semiconducting spin bands and thus half-metallic ferromagnets show one hundred percent spin-polarization at the Fermi energy [12]. The spin band of metallic part of half-metallic ferromagnet contacts forms a Schottky junction with the semiconductor channel, and the spin band of insulating part forms an energy barrier that its barrier height is proportional to the band gap of the insulating spin band. Thus, the spin-dependent barrier structure appears at the source and drain junctions as it is shown in Figure 6 (c). Another way to realize spin field-effect transistor is to employ tunnel junctions for the ferromagnetic source and drain [13]. So far different kinds of ferromagnetic semiconductors, ferromagnetic metals, and half-metallic ferromagnets have been used for the ferromagnetic electrodes of the tunnel junctions.

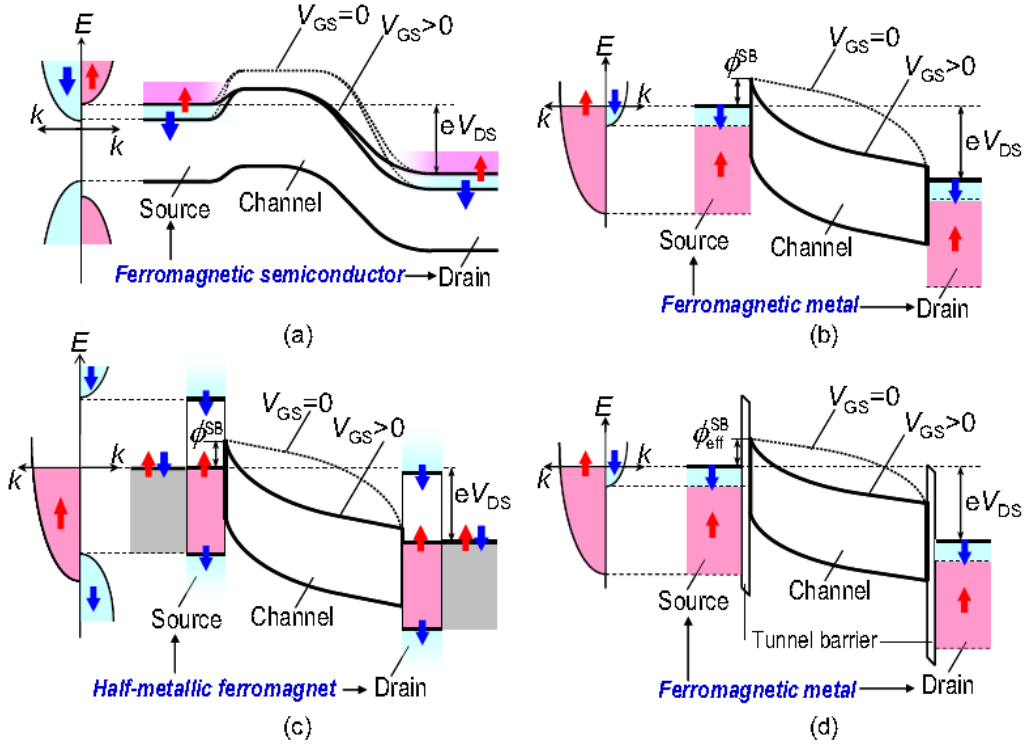

Figure 6 | Band diagrams of spin field-effect transistor with (a) ferromagnetic semiconductor source/drain, (b) ferromagnetic metal source/drain, (c) half-metallic ferromagnet source/drain, and (d) ferromagnetic tunnel contact source/drain [12].

When a metallic ferromagnet or a half-metallic ferromagnet is used for the ferromagnetic electrodes of the source or drain, the energy difference between the Fermi energy of the metallic or half-metallic ferromagnet and the conduction band edge of the channel act as an effective Schottky barrier (φ_{eff}^{SB} shown in Figure 6 (d)). Therefore, control of the effective Schottky barrier height instead of tunnel barrier height or thickness is very essential even for the tunnel junction contacts in order to tune the junction contact resistance. A spin field-effect transistor can also be comprised of a metal oxide semiconductor gate with a ferromagnetic semiconductor channel and ferromagnetic Schottky junctions for both the source and drain [14].

2.3 Device Structures of Spin Field-Effect Transistor

Ferromagnetic metals are the best candidates for making room temperature spin field-effect transistor source and drain contacts. However, as it was discussed earlier, conductivity mismatch between ferromagnetic metal contacts for source and drain hampers the spin injection into the channel and spin detection in drain. When we are dealing with diffusive electron transport in the channel, the much lower resistivity of the ferromagnetic metal in source or drain compared to that of the channel causes the almost same drop of the electrochemical potentials over the channel for both spin-up and spin-down electrons which cannot ensure efficient spin injection. Therefore, spin-dependent interfacial contact resistance (at the source or drain junctions) which is sufficiently larger than the channel resistance is required for efficient spin injection [15]. This increase in interfacial contact resistance decreases the overall device performance as it lowers the total conductance of the transistor device. Since the channel resistance in the *on*-state can be reduced with decreasing the channel length, the spin-dependent contact resistance should also be reduced with decreasing the channel length. Schottky junctions that use very thin low work function interfacial layers are promising junctions [16] since they can be further down scaled while still maintaining contact resistance character necessary for spin-dependent current injection.

Conductivity mismatch problem in the ballistic transport regime is considered to be non-relevant, because the resistance of the channel can be assumed zero. But we know that there is a large contact resistance at the source and drain junctions in the ballistic transport regime. This contact resistance deals with the output current and not that of the channel resistance, and hence the conductivity mismatch problem exists even in the ballistic regime [17]. Therefore, spin-dependent contact resistance is required for both diffusive transport and ballistic transport regimes. Since the resistivity of the ferromagnets is comparable to that of the channel, it rules out conductivity mismatch problem [12] and therefore ferromagnetic semiconductors are attractive candidates for source and drain materials. Other possible candidates may are half-metallic ferromagnet contacts with the spin-polarization of 100 % [12] for the source and drain contacts. Although in this case the tuning of the contact resistance would not be needed, the reduction of the Schottky barrier height is still required in order to have a good device performance.

Two device structures for spin field-effect transistors are shown in Figure 7. We call these structures bulk spin field-effect transistor and silicon on insulator (SOI) spin field-effect transistor corresponding with their configurations. Low production cost for bulk spin field-effect transistors and

excellent device performance for SOI spin field-effect transistors is expected [12]. In the bulk spin field-effect transistor, the ferromagnetic source or drain act as *electrical contacts* to the channel when the transistor is working in its *on*-state, and they work as *blocking contacts* for leakage current between the source and drain when the transistor is in its *off*-state.

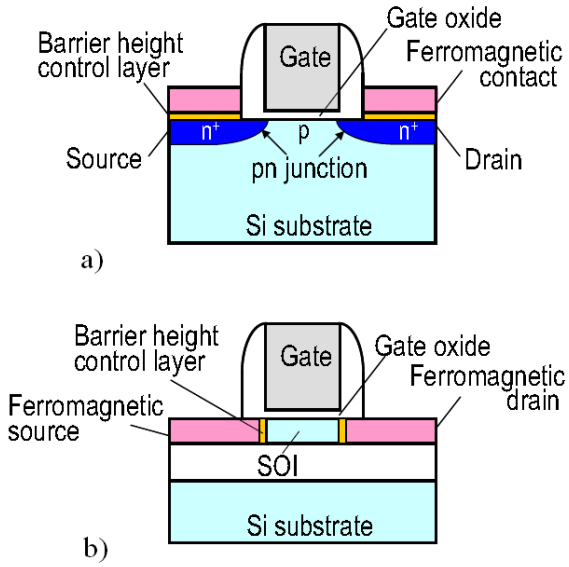

Figure 7 | Possible device structures of (a) bulk spin field-effect transistor and (b) Silicon on insulator (SOI) spin field-effect transistor [12].

Again considering the problem of conductivity mismatch, we see that p-n junctions which use a ferromagnetic semiconductor are the most suitable structures for the ferromagnetic source and drain configurations. On the other hand, Schottky junctions that use a ferromagnetic metal are also applicable to the ferromagnetic source or drain structures. We should note that in the bulk spin field-effect transistor, relatively high junction leakage current would be problematic for the Schottky junction contacts. Since the SOI spin field-effect transistor structure considerably minimize the junction area of the source and drain, this device structure is preferable for Schottky junction contacts. The dopant segregation effect during the formation of ferromagnetic silicides and the auto doping effect of epitaxial ferromagnetic metals which are grown on *Si* [18] are also effective to a large extent in reducing the junction leakage current of the ferromagnetic metal source and drain even in the bulk spin field-effect transistor structures.

One possible device structure of a spin field-effect transistor using nonmagnetic p-n junctions for the source and drain, where ferromagnetic metal or half-metallic ferromagnet contacts are formed on or inside the source and drain regions is shown in Figure 7 (a) (in this figure n^+ means highly n-doped). Tunnel contacts due to the Schottky junctions between the ferromagnetic metal and n^+ region can be used to remove the conductivity mismatch problem. Work function engineering using both an ultrathin interfacial insulating layer and an ultrathin low work function metal layer deposited on it to control the Schottky barrier height [16] is more likely to achieve the ferromagnetic contacts of source and drain. Since, SiO_2, Si_3N_4, and Al_2O_3 induce only a small density of interface states [12], these materials are promising candidates for interfacial insulating layers. Other prospective materials for the realization of an efficient, high spin injection rate are CoFe/MgO, CoFeB/MgO, and Heusler-alloy/MgO with a low work-function metal layer [12] placed at interfacial barrier to control barrier height.

Another possible device structure of a spin field-effect transistor which uses a thin semiconductor on insulator (SOI) structure is schematically shown in Figure 7 (b). The p-n junction based on ferromagnetic source or drain structures shown in Figure 7 (a) can be also applied to the SOI spin field-effect transistor structure while ferromagnetic Schottky junctions are themselves an alternative candidate. The thin body SOI

spin field-effect transistor structure provides several adjustable options in order to improve the device performance. In this configuration even when the ferromagnetic source and drain are in the form of Schottky junctions, the junction leakage current can be considerably reduced due to the extremely small junction area. Furthermore, a lower degree of doping for the channel or an intrinsic channel can be used in this device structure, which plays an essential role to exclude or minimize scattering of spin-polarized electrons that are transported through the channel. These characteristics show that in short SOI channels the ballistic transport of spin-polarized electrons can be expected.

To tune the contact resistance, silicidation reaction can be used to form the ferromagnetic source and drain [19]. In other words the dopant segregation effect during the silicidation in this case is helpful. The other promising way to control the contact resistance is to create Schottky junctions using low work function materials which are placed next to interfacial insulating layer.

3 Some Recent Advances in Spin Injection, Transport, and Detection

3.1 Spin Injection into Silicon

One of the successful works on injecting spin-polarized electrons from a ferromagnet into the silicon channel has been done by B. T. Jonker et al. [20]. They could successfully inject spin-polarized current from a ferromagnetic iron film through an Al_2O_3 tunnel barrier into *Si* (001) n-i-p doped hetero-structure.

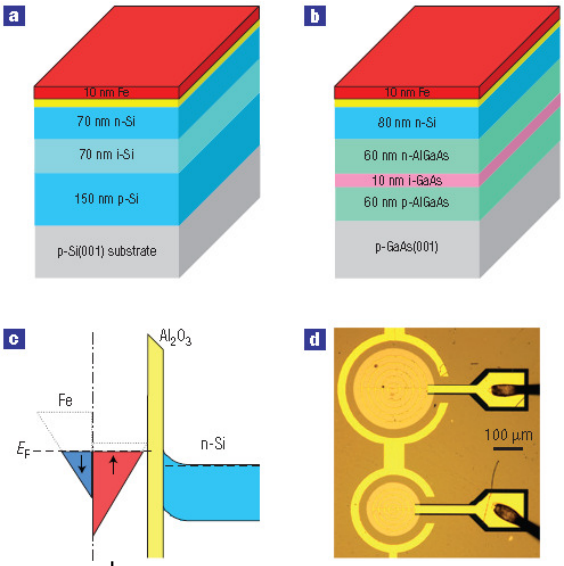

Figure 8 | (a, and b) When electrons are injected from the *Fe* contact under electrical bias, radiative recombination is observed as the electrons recombine with unpolarized holes in either the *Si* (n-i-p structure) (a) or the *GaAs* quantum well, Si/AlGaAs/GaAs/AlGaAs structure (b). (c) Band diagram showing the exchange split bands of the *Fe* contact, with majority spin electron states highlighted in red (up arrow) and minority spin states highlighted in blue (down arrow). (d) Photograph of processed light emitting diode (LED) structures. The circular plates are the active light emitting areas, the contact metallization appears in yellow and the wire contacts appear to the right [20].

The circular polarization of the electroluminescence resulting from radiative recombination in *Si* and *GaAs* structures was a signature of the existence of spin-polarization current in semiconductor originating from *Fe* magnetization.

They determined a *30%* difference between majority and minority spins before radiative recombination with unpolarized holes in *Si* happens at *5 K*. they observed the difference in majority and minority spin-polarization at temperatures of up to *125 K*. These results were confirmed by repeating the same experiments on $Fe/Al_2O_3/Si/AlGaAs/GaAs$ quantum well structures in which the spin-polarized electrons flow under applied field from the Si, and recombine later in the *GaAs* quantum well, where the polarized electroluminescence can be quantitatively analyzed (the schematic representation of these two structures are shown in Figure 8).

In Figure 9 electroluminescence spectra from a $Fe/Al_2O_3/Si$ n–i–p structure are shown for *5, 50, and 80* K. these electroluminescence data are analyzed for both $\sigma+$ (right handed) and $\sigma-$ (left handed) circular polarizations. At *5 K*, three peaks can be seen which arise from electron hole recombination accompanied by transverse acoustic (TA) or transverse optical (TO) phonon emission in the p-doped *Si* layers. These peaks are detected at *1.105 meV* associated with transverse acoustic, *1.09 meV* associated with TO-TA, and finally *1.05 meV* associated with TO+TA. At higher temperatures transverse acoustic related features are diminished as it can be seen in Figure 9 (b). Here we can see that the transverse optical feature occurring at *1.07 meV* dominates both temperatures of *50* and *80 K*.

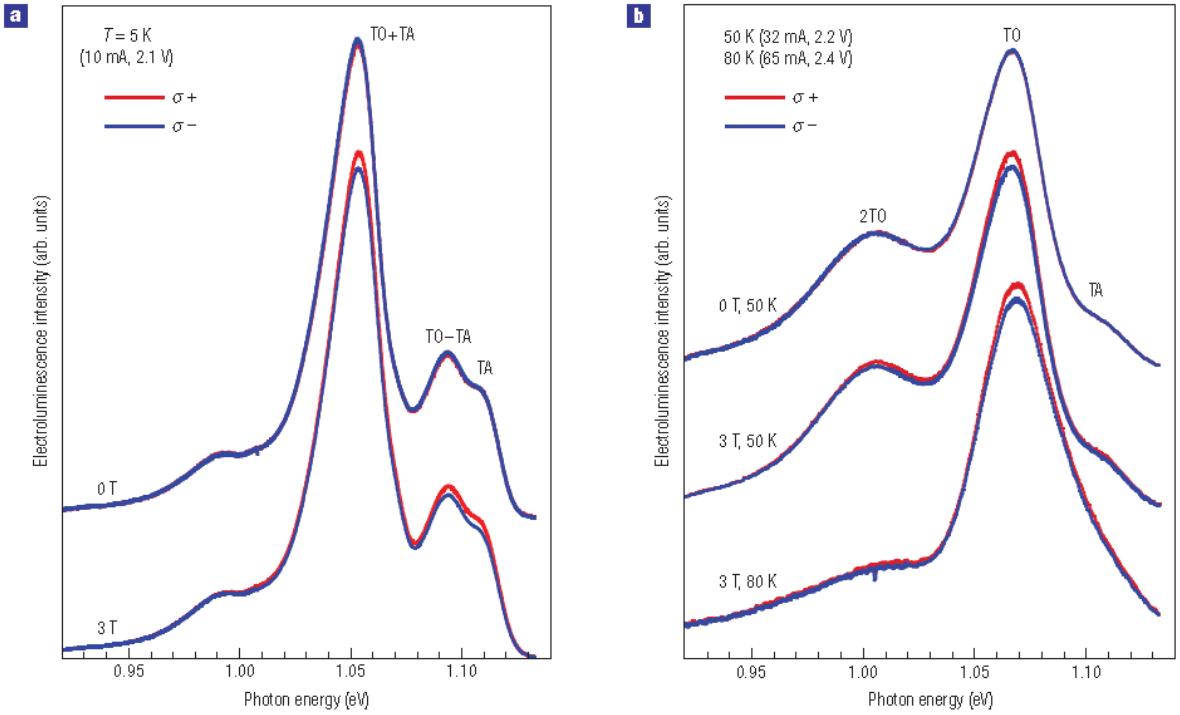

Figure 9 | (a, and b) Electroluminescence spectra at zero field and 3 T, analyzed for σ+ (red) and σ- (blue) circular polarization, for *T =5 K* (a) and *T =50* and *80 K* (b). The σ+ and σ- traces are coincident at zero fields, whereas the net polarization is clearly observed at *3 T* up to *80 K*. The magnetic field is applied perpendicular to the surface (parallel to the direction of light propagation) [20].

It also can be understood from Figure 9 that at zero magnetic fields, no circular polarization can be observed. This is because the *Fe* magnetization and corresponding electron spin orientation lie in plane and perpendicular to the light propagation direction. Therefore, although the spin injection may occur, it cannot be detected with this specific alignment. To overcome this obstacle B. T. Jonker et al. applied a magnetic field to rotate the *Fe* magnetization direction out of plane, and consequently all spectral lines showed circular polarization. This behavior is shown in Figure 9 by the difference between red (σ+) and blue (σ-) curves in three Tesla spectra for different temperatures of *5, 50,* and *80 K*.

3.2 Tunable Spin Tunnel Contacts on Silicon

As we discussed in the first chapter, one way to overcome the problem of conductivity mismatch is to incorporate a very thin layer of a low work function ferromagnet between ferromagnet contacts and insulator. On this basis Min and Jansen presented an experiment in which they could control spin tunneling resistance [16]. They incorporated a very thin layer of *Gd* at the interface between ferromagnet and tunnel barrier. Using this technique they could show that the resistance-area product of ferromagnet/Insulator/Si (FM/I/Si) contacts was tunable over eight orders of magnitude, while at the same time maintaining a reasonable tunnel spin-polarized injection into the *Si* based semiconductor.

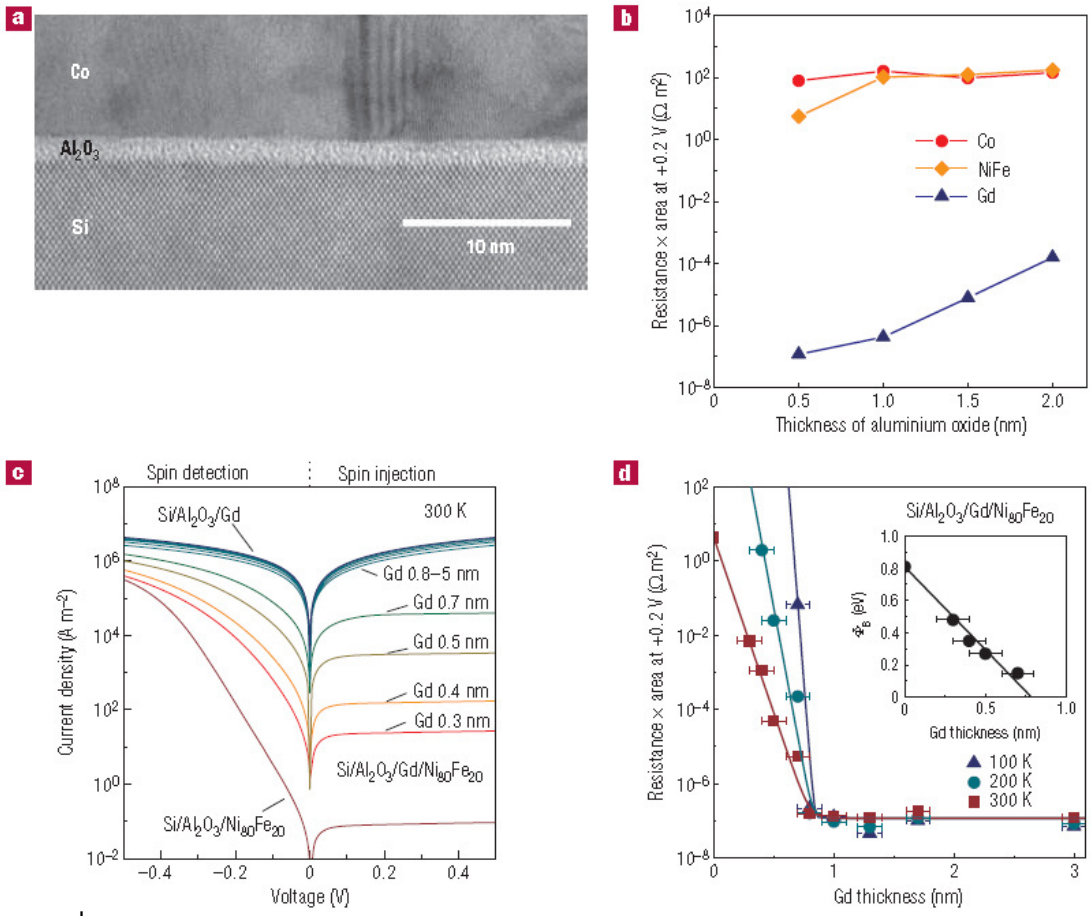

Figure 10 | (a) Cross-sectional transmission electron micrograph of $Si/Al_2O_3/Co$ contacts. (b) Resistance-area product of the tunnel contact at the reverse bias of *+0.2 V* versus the thickness of the Al_2O_3 tunnel barrier. The red data is for the $Si/Al_2O_3/Co$ ($Ni_{80}Fe_{20}$) (*15nm*) contacts, the blue data is for the $Si/Al_2O_{3s}/Gd$ (*15 nm*) contacts. (c) Absolute value of current density versus bias voltage of Si/Al_2O_3 (*0.5nm*)/$Ni_{80}Fe_{20}$ (*15 nm*), Si/Al_2O_3 (*0.5nm*)/Gd (*15 nm*) and Si/Al_2O_3 (*0.5nm*)/Gd (*0.3–5 nm*)/$Ni_{80}Fe_{20}$ contacts. The minus voltage is the forward bias (the spin detection condition); the positive voltage is the reverse bias (the spin injection condition). (d) Resistance-area product of the Si/Al_2O_3 (*0.5nm*)/Gd/$Ni_{80}Fe_{20}$ (*10 nm*) contacts at a reverse bias of *+0.2 V* versus the thickness of the Gd interlayer. The inset shows the Schottky barrier height of the contact versus the thickness of the *Gd* interlayer. The error bars denote the accuracy of the determination of the *Gd* thickness [16].

The Schottky barrier height of a FM/I/Si contact is determined by the work function of the metal, the electron affinity of *Si* and the number of surface states at the *Si* surface [21]. The Schottky barrier height can be decreased using a material with a work function lower than that of *Co*, *Ni*, or *Fe* [22], while the material should still be ferromagnetic to have the ability to inject spin-polarized electrons into the *Si* channel. They used *Gd* as the low work function ferromagnetic material to control the resistance-area product of spin tunnel contacts.

In their experiment ferromagnet-insulator-semiconductor (FM/I/Si) contacts were fabricated with well-known ferromagnetic materials, *Co* and $Ni_{80}Fe_{20}$. Figure 10 (a) shows a cross-sectional transmission electron micrograph of a $Si/Al_2O_3/Co$

contact on low doped n-type *Si* substrates. The resistance-area product of the contact is defined as the voltage, *V,* divided by the current density, *I/A,* at a particular value of *V*. The resulting resistance-area product for this configuration was about eight orders of magnitude higher than the value needed for efficient spin injection.

When an ultrathin layer of *Gd* is used between ferromagnet and insulator, the resistance-area product of the Si/Al_2O_3/Gd contact reaches the optimum range in Figure 10 (b) for both spin injection and spin detection contacts. The resistance-area product of the contact with a *Gd* layer shows an exponential dependence on the barrier thickness as it can be seen in this figure. It means that the dominant transport mechanism across the Al_2O_3 barrier in this case is the tunnel transport.

Figure 10 (c) shows the *I–V* characteristics of a Si/Al_2O_3*(0.5 nm)*/$Ni_{80}Fe_{20}$ and a Si/Al_2O_3*(0.5nm)*/Gd tunnel contact on low doped *Si*. As it is shown in this figure, the current density of the Si/Al_2O_3/$Ni_{80}Fe_{20}$ contact is very small in the reverse bias range and it only has a small dependence on the voltage. In contrast, the current density of the Si/Al_2O_3/Gd tunnel contact in the reverse bias range is more than seven orders of magnitude larger than the current density for Si/Al_2O_3/$Ni_{80}Fe_{20}$. We can also see from this figure that the current density of the Si/Al_2O_3/Gd tunnel contact in the forward bias range is considerably increased. Therefore, the *I–V* curves of contacts with *Gd* show symmetric behavior, which is important in obtaining the same resistance-area product for source and drain contacts.

The resistance area product of the tunnel contacts decreases suddenly by increasing the thickness of the *Gd* interlayer and saturates to the resistance area product of the FM/I/Si contact when *Gd* interlayer is *15 nm*. This situation is shown in Figure 10 (d) and as it can be seen the resistance-area product for a *1 nm Gd* interlayer, for the case of spin injection condition (*V =+0.2 V*), is reduced by about eight orders of magnitude. Similar behavior occurs for the resistance area product in the case of spin detection (negative bias). When the thickness of the Gd layer is more than about *1 nm*, the resistance area product of the contact at a constant value saturates. This is because when the thickness of *Gd* is *1 nm,* the surface coverage of the *Gd* is complete [16] (we know that the work function is sensitive to the outermost surface layers of a material). Also it can be seen that temperature dependence still remains for the tunnel contacts with a *Gd* interlayer thinner than *0.7 nm*. At the same time we see that, this temperature dependence disappears for the tunnel contacts with a *Gd* interlayer thicker than *1.0 nm* (for which the Schottky barrier is removed).

3.3 Spin Transport in GaAs

One of the most remarkable works on electrical detection of spin transport in ferromagnetic-semiconductor devices was done by P. A. Crowell et al. [23] in 2007. They demonstrated a fully electrical scheme for achieving spin injection, transport and detection in a *GaAs* based device. Since optical spin detection methods are very successful in *GaAs* the electrical experiments in their work could be verified by optical means. Their device, as it is shown in Figure 11, consisted of a main semiconductor channel with several ferromagnetic contacts. Considering different experiments, relevant contacts were used as source and drain to measure both local (when the same contacts are used as voltage application and detection) and non-local (when different contacts are used as voltage application and detection) spin-polarizations of the electrons.

In a non-local spin sensitive current detection, Schottky tunnel barrier contact's electrochemical potential depends on the relative magnetizations of the source and drain (drain here is called detector). They verified the effectiveness of their device configuration by showing the existence of Hanle effect (in Hanle effect a transverse magnetic field suppresses the non-local signal at the detection contact by inducing spin precession and dephasing in the channel). The output signal was varying with the injection current and was correlated with the spin-polarization in the channel.

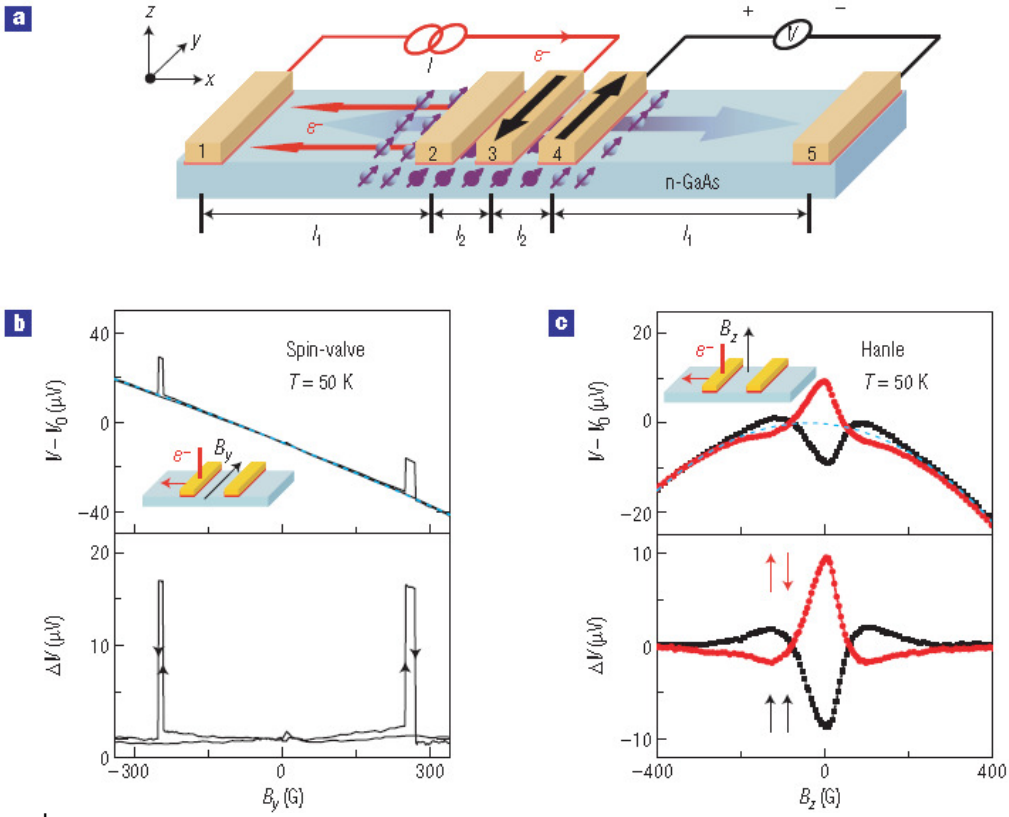

Figure 11 | (a) A schematic diagram of the non-local experiment configuration. Five *10×50 μm Fe* contacts have their magnetic easy axes along $\hat{y}$, which is in [011] direction of the GaAs. The large arrows on *Fe* contacts indicate the magnetizations of the source and detector. Length of the two main channels and distance between *Fe* contacts are l_1 =160 μm and l_2 =12 μm, respectively. Electrons are injected along the direction that is shown in red. The injected spins (purple) diffuse in either direction from contact 3 and the non-local voltage is detected at contact 4. (b) A non-local voltage, $V_{4,5}$, versus in-plane magnetic field B_y which is swept in both directions at a current of $I_{1,3}$ =1.0 mA at T=50 K, can be seen. The raw data are shown in the upper panel with an offset V_0=-30.227 mV subtracted. The background here is shown as dashed cyan curve underneath the data and is fitted by a second order polynomial. The lower shows the data while this background data is subtracted. (c) Another non-local voltage, $V_{4,5}$, but this time magnetic field is in the direction of z (B_z) for the same contacts and bias conditions and the same offset V_0 as in part (b). The dashed cyan curve data in the lower panel again is the upper panel raw data subtracted by background data. The data that are shown in black are obtained with the magnetizations of contacts 3 and 4 parallel while the data shown in red are obtained in the anti-parallel configuration [23].

The interpretation of electrical spin-transport measurements can be complicated by background effects (background effects include magneto resistance in the electrodes, local Hall effects and other extrinsic contributions to the signal). A non-local measurement minimizes these background effects by placing a spin detection electrode outside the path of the charge current.

Figure 11 (a) shows a schematic diagram of the non-local experiment configuration that was used in this experiment. In this figure the magnetic easy axes of five *10×50 μm Fe* contacts are at $\hat{y}$ direction (i.e., in [011] direction of the GaAs). The large arrows on *Fe* contacts indicate the magnetizations of the source and detector. Length of the two main channels and distance between *Fe* contacts are l_1 *=160 μm* and l_2 *=12 μm*, respectively. Electrons are injected along the direction that is shown in red. The injected spins (purple) diffuse in both left and right directions from contact 3 and the non-local voltage is detected at contact 4.

The data in Figure 11 (b) indicates the existence of a lateral spin-valve effect. In this figure non-local voltage, $V_{4,5}$, versus in-plane magnetic field B_y which is swept in both directions at a current of $I_{1,3}$ *=1.0 mA* at *T*=50 K, is presented. The raw data are shown in the upper panel with an offset V_0*=-30.227 mV* subtracted. The background here is shown as dashed cyan curve underneath the data and is fitted by a second order polynomial. Lower part of this figure shows the data while this background data is subtracted. Two squares jump with a magnitude of *16.8±0.2 μV* and occur in a field range in which the magnetizations of contacts 3 and 4 are anti-parallel.

What is most significant in their work is the fact that previous measurements done by other research groups on devices having ferromagnetic-semiconducting contacts, had not demonstrated precession of the spin on their way from source to drain. To investigate this property they used the Hanle effect [24], in which the magnetic field dependence of the non-local voltage was due to precession and dephasing of the spins in the semiconductor channel. The precession was induced by applying a small transverse magnetic field to the extent that it could not change the magnetizations of the electrodes. In their experiment they set the magnetizations of contacts 3 and 4 in parallel and the external magnetic field in the direction of B_z. the magnetic field then swept through the range *-400 G* to *400 G* resulting in the black data points shown in the top panel of Figure 11 (c). The offset V_0 is the same as for Figure 11 (b). The corresponding data after subtraction of the background are shown here as dashed cyan lines in the lower panel of Figure 11 (c). This procedure was repeated for anti-parallel configuration of contacts 3 and 4 which resulted in the red data points in Figure 11 (c). It can be seen from this figure that the two Hanle curves coincide at large B_z as in this limit the electron spins in the *GaAs* channel are completely dephased. The difference in two Hanle signals at *B = 0* is *18.0±0.1 μV*, which is different from the jump in the spin-valve data by an amount of *1.2 μV*.

3.4 Spin Transport in Silicon

Earlier we discussed how Crowell et al. [23] could measure and verify the spin transport across a channel of *160 μm* in *GaAs*. Since the mainstream industry is based on silicon technology, it is very important if we can find a way to transport spin-polarized electrons across long distances in silicon.

Along with the realization of this goal, I. Appelbaum et al. [25] conducted a successful experiment and measured a controlled spin transport in silicon. They could transport and measure a spin-polarized current across *10 μm* undoped *Si* in a

ballistic transport regime. The silicon was sandwiched between ferromagnetic thin films for both spin injection and spin detection. The hot electron (a hot electron is an electron which is not in thermal equilibrium with its semiconducting environment) spin injection and spin detection that was used in their experiment avoided resistance mismatch between ferromagnetic and semiconducting layers. A schematic representation of this device is shown if Figure 12.

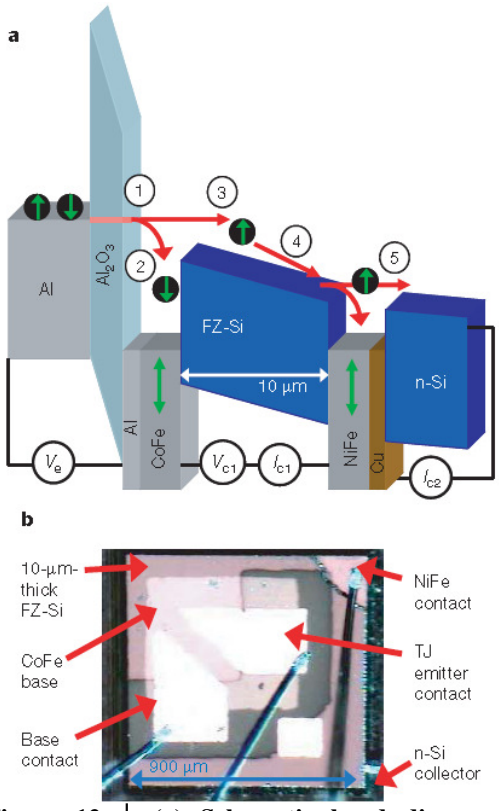

Figure 12 | (a) Schematic band diagram. At constant emitter voltage (V_e), the *first collector current* (I_{c1}) is measured at the *NiFe* contact and *second collector current* (I_{c2}) is measured at an *In* contact to the n-doped *Si* substrate, under optional voltage bias (V_{c1}) across the single crystal undoped float zone *Si* (FZ-Si) drift region. (b) A top down micrograph of a representative wire bonded *Si* spin transport device it shows the device structure, contacts to the tunnel junction base and emitter, and spin detector buried *NiFe* layer [25].

In step 1, unpolarized electrons are injected from *Al* emitter into the ferromagnetic $Co_{84}Fe_{16}$ through tunnel junction and create emitter current I_e. In step 2, the flow of minority spin electrons is attenuated through scattering. In step 3, majority electrons which have their spins parallel to the magnetization of $Co_{84}Fe_{16}$ are transported over Schottky barrier into float zone (FZ) and form the first collector current I_{c1}. In step 4, the majority spin-polarized current makes its way through $10\,\mu m$ undoped Si. In step 5, second collector current I_{c2} (magnitude of I_{c2} depends on the relative magnetization direction of both ferromagnetic layers) is formed from ballistic transport through ferromagnetic $Ni_{80}Fe_{20}$ into n-doped *Si* substrate. When magnetizations of the two ferromagnetic layers are parallel, I_{c2} is higher than when the magnetizations are anti-parallel.

In Figure 13 in-plane magnetic field dependence of second collector current (I_{c2}) at V_e=*-1.8 V* and *85 K* is shown. Measurements begin from the far ends of the figure when the magnetization directions of two ferromagnets are parallel. When the magnetic field is swept through zero it changes sign and first forces the magnetization of $Ni_{80}Fe_{20}$ to switch (in the direction of applied field) so that the magnetization directions of ferromagnets are anti-parallel. This results in a reduction in I_{c2} of approximately two percent. By further increasing the magnetic field strength, the magnetization direction of $Co_{84}Fe_{16}$ is also aligned with the applied magnetic field direction. In this way again higher collector current (I_{c2}) is obtained. The symmetric magnetic field dependence of I_{c2} upon reversal of sweep direction in Figure 13 indicates that the electron spin maintains polarization while travelling through *10 µm* thick of float zone silicon.

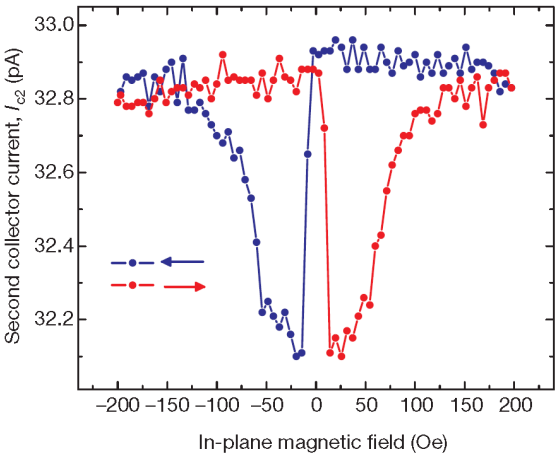

Figure 13 | In-plane magnetic field dependence of second collector current (I_{c2}) at constant emitter bias V_e=-1.8 V and V_{c1}=0 V, showing an approximate two percent *spin valve* effect at *85 K* [25].

Dependence of I_{c2} on external magnetic field which is perpendicular to the film plane (while V_{c1}=0 V) is shown in Figure 14 (a). The measurement begins with the field at *-5 kOe*, where a small in-plane component orients the in-plane $Ni_{80}Fe_{20}$ and $Co_{84}Fe_{16}$ magnetizations parallel to each other. Following the red line to the right towards smaller field values, a peak near *-0.7 kOe* and a dip near *-0.35 kOe* can be seen. Once the magnetic field is past zero, the small in-plane component of magnetic field switches the $Ni_{80}Fe_{20}$ magnetization which causes an anti-parallel magnetization direction of source and drain. By reversing the external magnetic field scan direction (blue line) a similar feature is obtained.

If the precession of spin direction in the external magnetic field is to the extent that when it arrives at the $Ni_{80}Fe_{20}$ thin film, it is parallel to the magnetization direction of this film, a maximum is observed in the I_{c2} current. On the other hand, if the precession of spin direction in the external magnetic field is to the extent that at the vicinity of the magnetic thin film it is oriented anti-parallel to the magnetization direction of $Ni_{80}Fe_{20}$ thin film, a minimum is observed in the I_{c2}.

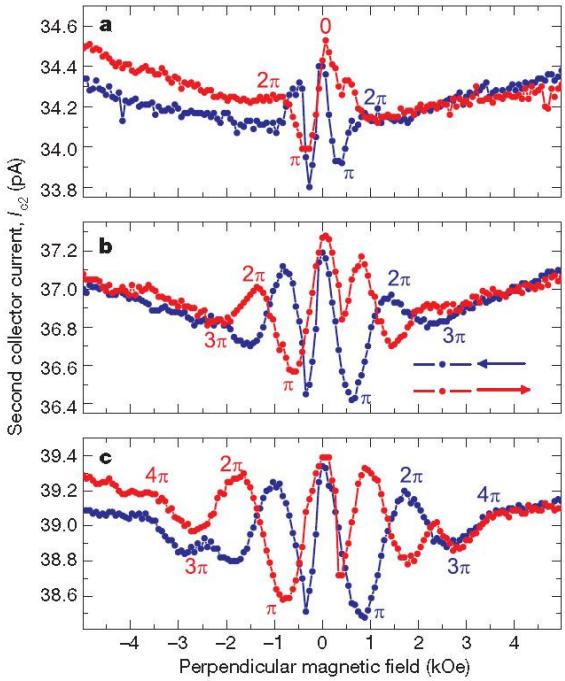

Figure 14 | (a) Second collector current, I_{c2}, in zero applied voltage V_{c1}. (b and c) Like part (a) but under an accelerating voltage bias of *0.5 V* (b) and of *1.0 V* (c). At higher accelerating voltages, the spin-polarized electron transport time is reduced in the increased drift field, so the precession angle at fixed magnetic field is smaller, causing an increased precession period and revealing the presence of precession angles up to *4π*. In this experiment magnetic field has been perpendicular to the direction of spin-polarized current inside the channel at constant emitter voltage of V_e=-1.8 V and *85 K* [25].

When the electric drift field is increased with an applied voltage bias, V_{c1}, the transmission time is reduced, and the precession angle at any fixed magnetic field is consequently reduced. This pushes the maxima and minima to higher values of perpendicular magnetic fields. These behaviors are shown in Figure 14 (b) and (c) for V_{c1}=0.5 V and V_{c1}=1 V accelerating voltages, respectively. Under these higher accelerating electric fields, drift is even more dominant than in Figure 14 (a) and precession angles up to *4π* can be seen.

4 Conclusion

If realized, the spin field-effect transistor will provide many benefits as being smaller, quicker, using lower power, and generating lower heat than the present charge based transistors. However, in order to reach the point in which spin field-effect transistor is fully operational, there are some challenges which need to be overcome. We can categorize all these challenges into four main classes, viz. spin injection, spin transport, spin detection, and spin manipulation.

We have seen how various research groups have successfully overcome problems of conductivity mismatch between ferromagnets and semiconductors using different approaches. We have also seen how some of these groups have addressed issues regarding spin diffusion time and spin diffusion length of electrons in the semiconductor channel. Based on what we have seen in this article we now know that challenges like spin injection, spin transport, and spin detection in semiconductors all have been successfully addressed and overcome by different groups.

Nevertheless, these achievements does not mean that all the problems on the way of making spin field-effect transistor have been solved. This would become more obvious when we look more closely into the recent works which were described in the last chapter. Most of the experiments described, operate in very low temperatures making it an open challenge to realize room temperature injection of spins in semiconductors. And as we know one of the main objectives in the field of Spintronics is to make room temperature spin field-effect transistor devices. Another problem which can be seen in the most promising three terminal device made by Appelbaum *et. al.* is that it has low output current thus making the detection of spin-polarized current difficult at the drain contact. The other problem on the way of making spin field-effect transistor arises from the combination of ferromagnetic materials with semiconductors which gives rise to many different compatibility problems. The mentioned problems might still not be the most significant ones on the way of realization of the spin field-effect transistor, but the most significant challenge might be to introduce the gate contact by which spins inside the semiconductor channel can be manipulated.

In this article we have followed the progressive trend towards the realization of spin field-effect transistor after it was first proposed by Datta and Das almost two decades ago. Now we come back to the question that was raised at the beginning of this article. Can the spin field-effect transistor be realized? The answer to this question is *yes*. Despite various problems on the way of the spin field-effect transistor realization, significant achievements by various groups in especially the last two years gives hope that the realization of the *spin field-effect transistor*, though challenging can be within reach.

5 Acknowledgments

In the end I want to express my sincere gratitude to both Caspar van der Wal and Tamalika Banerjee from Zernike Institute for Advanced Materials whose kind consultations led me through all difficulties while writing this article.

6 References

1 M. N. Baibich, J. M. Broto, A. Fert et al., "Giant Magnetoresistance of (001)Fe/(001)Cr Magnetic Superlattices," Physical Review Letters 61, 2472-2475, (1988).

2 G. Binasch, P. Grunberg, F. Saurenbach et al., "Enhanced Magnetoresistance in Layered Magnetic-Structures with Antiferromagnetic Interlayer Exchange," Physical Review B 39, 4828-4830, (1989).

3 J. Daughton, J. Brown, E. Chen, R. Beech, A. Pohm, and W. Kude, "Magnetic field sensors using GMR multilayer," IEEE Trans. Magn., vol. 30, no. 6, 4608-4610, (1994).

4 S. Datta and B. Das, "Electronic analog of the electro-optic modulator," Appl. Phys. Lett. vol. 56, 665-667, (1990).

5 J. S. Moodera, L. R. Kinder, T. M. Wong, and R. Meservey, "Large magnetoresistance at room temperature in ferromagnetic thin film tunnel junctions," Phys. Rev. Lett. vol. 74, no. 16, 3273–3276, (1995).

6 W. H. Meiklejohn and C. P. Bean, "New magnetic anisotropy," Phys. Rev. vol. 102, no. 5, 1413-1414, (1956).

7 G. Schmidt, D. Ferrand, L. W. Molenkamp et al., "Fundamental obstacle for electrical spin injection from a ferromagnetic metal into a diffusive semiconductor," Physical Review B vol. 62, R4790-R4793, (2000).

8 International Technology Roadmap for Semiconductors. Semicond. Ind. Assoc., San Jose, CA. [Online: http://www.itrs.net/Links /2003ITRS/PIDS2003.pdf], (2003).

9 M. E. Flatte, "Spintronics," IEEE Transactions on Electron Devices vol. 54, no. 5, 907-920, (2007)

10 R. Landauer, "Irreversibility and heat generation in the computing process," IBM J. Res. Develop. vol. 5, no. 3, 183-191, (1961).

11 K. Hall, W. H. Lau, K. Gundogdu, M. E. Flatte, and T. F. Boggess, "Nonmagnetic semiconductor spin transistor," Appl. Phys. Lett. vol. 83, no. 14, 2937-2939, (2003).

12 S. Sugahara, "Perspective on field-effect spin-transistors," phys. stat. sol. no. 12, 4405-4413, (2006).

13 S. Sugahara and M. Tanaka, "Spin MOSFETs as a basis for spintronics," ACM Transactions on Storage no. 2, 197, (2006).

14 S. Sugahara and M. Tanaka, "A spin metal-oxide-semiconductor field-effect transistor (spin MOSFET) with a ferromagnetic semiconductor for the channel," J. Appl. Phys. vol. 97, 10D503, (2005).

15 A. Fert and H. Jaffres, "Conditions for efficient spin injection from a ferromagnetic metal into a semiconductor," Phys. Rev. B vol. 64, 184420, (2001).

16 B. C. Min, and R. Jansen et al., "Tunable spin-tunnel contacts to silicon using low-work-function ferromagnets," Nature Materials vol. 5, 817-822, (2006).

17 V. Y. Kravchenko and E.I. Rashba, "Spin injection into a ballistic semiconductor microstructure," Phys. Rev. B vol. 67, 121310, (2003).

18 K. Sugiura, R. Nakane, S. Sugahara, and M. Tanaka, "Schottky barrier height of ferromagnet/Si(001) junctions," Appl. Phys. Lett. vol. 89, 072110, (2006).

19 R. Nakane, M. Tanaka, and S. Sugahara, "Preparation and characterization of ferromagnetic DO_3-phase Fe_3Si thin films on silicon-on-insulator substrates for Si-based spin-electronic device applications," Appl. Phys. Lett. vol. 89, 192503, (2006).

20 G. Kioseoglou, A. T. Hanbicki, C. H. Li, P. E. Thompson, B. T. Jonker, "Electrical spin-injection into silicon from a ferromagnetic metal/tunnel barrier contact," Nature Physics vol. 3, 542-546, (2007).

21 S. M. Sze, Physics of Semiconductor Devices 2nd edition, Wiley, New York, (1981).

22 D. Connelly, C. Faulkner, P. A. Clifton, and D. E. Grupp, "Fermi-level depinning for low-barrier Schottky source/drain transistors," Appl. Phys. Lett. vol. 88, 12105, (2006).

23 P. A. Crowell, X. Lou et al., "lateral ferromagnet-semiconductor devices," nature physics vol. 3, 195-202, (2007).

24 F. J. Jedema, H. B. Heersche, A. T. Filip, J. J. A. Baselmans, and B. J. van Wees, "Electrical detection of spin precession in a metallic mesoscopic spin valve," Nature vol. 416, 713-716, (2002).

25 I. Appelbaum, B. Huang, D. J. Monsma, "Electronic measurement and control of spin transport in silicon," Nature vol. 447, 295-298, (2007).